Supplementary Information: "Bismuthates: $BaBiO_3$ and related superconducting phases"

Arthur W. Sleight

1. **Coexistence of *Ibmm* and *I4/mcm* phases**
2. **Tilt angle and distortion of MO_6 octahedra**

1. Coexistence of *Ibmm* and *I4/mcm* phases An understanding of relationships for the tetragonal (*I4/mcm*) and orthorhombic (*Ibmm*) phases in the $BaPb_{1-x}Bi_xO_x$ system is critical because these two phases generally coexist whenever superconductivity occurs in this system. Thus, other systems possessing transitions between these two space groups are reviewed here along with some related material. Orthorhombic space groups have different designations depending on their setting. Space group *Ibmm* is #74 in the International Tables for Crystallography. Some publications use other designations for this space group such as *Imma*, *Imcm*, and *Incn*.

A transition from *Ibmm* to *I4/mcm* is observed with increasing temperature at ~140 for $SrMoO_3$, at ~280 K for $BaTbO_3$, at ~560 K for $BaPbO_3$, at ~625 for $SrTcO_3$, at ~840 K for $SrRuO_3$, at ~1060 K for $SrSnO_3$, and at ~1110 K for $SrZrO_3$ (Figs. S1-S6) [1-7]. Apparently, these are the only known examples of this transition for simple AMO_3 compounds with the perovskite structure. Group theory analysis shows that this *Ibmm*-*I4/mcm* transition must be discontinuous (first-order) [8]. Thus, we expect some hysteresis of the temperature of the transition and also some coexistence of the *Ibmm* and *I4/mcm* phases over a small temperature range. In fact, the coexistence temperature range for all these known AMO_3 examples is small, less than ~15 degrees (Figs. S1-S6). For example in the case of $SrRuO_3$, only *I4/mcm* is observed at 838 K, both *I4/mcm* and *Ibmm* are observed at 828 K, and only *Ibmm* is observed at 823 K. The behavior of these seven examples is very different than that observed in $BaPb_{1-x}Bi_xO_x$ phases for values of *x* where superconductivity occurs. In the case of a $BaPb_{0.8}Bi_{0.2}O_3$ sample, coexistence of *I4/mcm* and *Ibmm* phases was observed from 4.2 to ~450 K [9].

Apparently, the only known cases of large coexistence ranges of *Ibmm* and *I4/mcm* perovskite phases occurs when there is more than one cation on either the A or M site. A good example is found in the $Sr_{1-x}Ba_xHfO_3$ system (Figs. S7-S9)[10]. Near x = 0.5, there is a significant range of coexistence of both the *Ibmm* and *I4/mcm* phases (Fig. S7). A common feature of discontinuous phase transitions in the simple AMO_3 perovskites is that the tilt angle and unit cell volume change in a nearly continuous manner through the transition, despite the significant jump in cell edges that occurs at this transition (Fig. S2). This greatly helps in understanding the results in systems such as $Sr_{1-x}Ba_xHfO_3$. Fig. S8 shows the volume fraction of the tetragonal phases as a function of temperature. As expected the volume fraction of the high-temperature tetragonal phase decreases with decreasing temperature. Fig. S9

shows the volume of the two units cells over the same temperature range. If the *Ibmm* and *I4/mcm* unit cells derived from the same composition, we would expect that the volumes from the two cells would nearly superimpose giving one curve with cell volume increasing with increasing temperature. The observed result can be explained on the basis that the *Ibmm* phase contains more Sr than the *I4/mcm* phase. As temperature decreases the Sr–rich regions of the *I4/mcm* phase progressively transform to the *Ibmm* phase, decreasing the relative amount of the *I4/mcm* phase. Thus for a nominal $Sr_{1-x}Ba_xHfO_3$ composition, *x* increases in the *I4/mcm* phase as temperature decreases. The larger Ba relative to Sr then compensates the anticipated thermal contraction, yielding a nearly flat dependence of volume for the *I4/mcm* phase with temperature. With decreasing temperature the *x* value in the *Ibmm* phase is decreasing relative to the nominal *x* value, and this causes the volume decrease with decreasing temperature to be greater than would otherwise be expected. In Fig. S7 lines have been added to show the expectation if equilibrium were achieved in the two phase region. The unit cell dimensions should be invariant in both the *Ibmm* phase and the *I4/mcm* phase. Only the relative amounts of the two phase should vary in this region. The experimental result suggests that the system is close to equilibrium.

In the $Sr_{1-x}Ba_xZrO_3$ system, no coexistence of *Ibmm* and *I4/mcm* was observed as a function of x or temperature (S10) [11].

Another system to consider is $(Ca,Sr,Ba)SnO_3$ (Fig. S11) [12]. With increasing average size of the A cation space groups *Pbnm*, *Ibmm*, *I4/mcm*, and $Pm\bar{3}m$ are observed. No coexistence region of *Ibmm* and *I4/mcm* was observed. However, diffraction patterns of samples in the region of space group *Pbnm* were only well fit by assuming two phases, both in space group *Pbnm* but with differing Ca/Sr ratios, most likely caused by lack of equilibration.

Perovskite $CeAlO_3$ has a *I4/mcm*-to-*Ibmm* transition with increasing temperature at about 400 K [13]. This transition is assumed to be related to the $4f^1$ electronic configuration of Ce^{3+}. No other AMO_3 perovskite compound is known to have such a transition. No region of coexistence of *I4/mcm* and *Ibmm* was detected. However, in the $Pr_{1-x}Sr_xMnO_3$ system there is also a *I4/mcm*-to-*Ibmm* transition with increasing temperature, and there is coexistence of the two phases as a function of *x* and temperature [14]. The reason for this unusual situation is not understood, but could be related to the charge ordering, orbital ordering, oxygen vacancies, and/or A site ordering.

We can conclude that the coexistence of *Ibmm* and *I4/mcm* phases for simple AMO_3 compounds with the perovskite structure only occurs over a small range of temperature, less than ~15 K. Such a coexistence range is expected given that these two phases are related be a discontinuous (first-order) transition. Such a transition is expected to have hysteresis and some coexistence range close to the transition

temperature. Once we have phases with mixed cations on one cation site, as in any solid solution, large ranges of coexistence of the *Ibmm* and *I4/mcm* phases are sometimes observed as function of temperature (more than 200 K) and composition. We can attribute this to compositional inhomogeneity, which does not occur in simple AMO_3 compounds. In the case of $Sr_{1-x}Ba_xHfO_3$ system, the results can be understood on the basis of Sr-rich and Ba-rich regions as discussed above. Such regions can occur for two very different reasons. Normally, such samples are prepared by reacting oxides of the three components. In the case of the $Sr_{1-x}Ba_xHfO_3$ study, these reactants were $SrCO_3$, $BaCO_3$, and HfO_2. These were mixed and heated to high temperatures where CO_2 was liberated as the perovskite phase formed. When the perovskite structure first forms, regions close to an original $SrCO_3$ reactant particle will be rich in Sr relative to the nominal composition. Likewise, regions close to an original $BaCO_3$ reactant particle will be rich in Ba. Once the perovskite structure is fully formed, the driving force for further reaction is very much diminished, and homogenization of Sr and Ba content may be very slow and require very long heating times at very high temperature. A better approach is sometimes to use precursor techniques that produce a reactant homogeneous with respect to Sr and Ba content before reacting with the Hf reactant. This is an example of inhomogeneity caused by failure to reach equilibrium. However, significant segregation of components sometimes occurs in well-equilibrated samples. When a complete solid solution between two components exists at high temperature, but a miscibility gap occurs on cooling, a precursor to phase separation will occur as the miscibility gap is approached from high temperature. Here some regions will be enriched by one component, and other areas will be enriched by the other component. Inhomogeneity produced by either of these routes can show its presence by broadening of peaks in diffraction patterns. This broadening is distinctly different than that caused by small crystallite size, and can be modeled as lattice strain.

Comparing the $BaPb_{1-x}Bi_xO_3$ system to the $Sr_{1-x}Ba_xHfO_3$ system we have some commonalities and some striking differences. In both cases, *Ibmm* and *I4/mcm* phases exist over a range of *x* values, and in both cases the volume percent of the *I4/mcm* phase decreases over a large temperature range. However, there are striking differences between these two systems. For the $Sr_{1-x}Ba_xHfO_3$ phases a decrease in the relative amount of *I4/mcm* phase was observed from room temperature down to ~50 K where it leveled off at about 7% (Fig. S8). In the case of a $BaPb_{0.8}Bi_{0.2}O_3$ sample, the relative amount of *I4/mcm* phase decreased from 100% at about 475 K, but it levels off at ~57% at ~275 K (Fig. 9 in main paper)[9]. Furthermore, over the entire temperature range of their coexistence (4.2 to 475 K), the volume of the unit cell of the *I4/mcm* phase is slightly larger than that of the *Ibmm* unit cell by the same amount (Fig. S12) [9]. This behavior and the behavior of the room temperature lattices constants of the two phases indicates that both the *Ibmm* and the *I4/mcm* phases have compositions close to the nominal composition for all values of *x*. Thus, the situation in the $BaPb_{1-x}Bi_xO_3$ and $Sr_{1-x}Ba_xHfO_3$ systems is actually very different. There are several possibilities for the anomalies of the

$BaPb_{1-x}Bi_xO_3$ system. One is that there really is something different about the Ibmm and I4/mcm phases in this case. This could, for example, be a different oxygen content or a different situation regard to Bi/Pb short range order. The other possibility is that lattice strain caused by twining and the intergrowth of the *Ibmm* and *I4/mcm* phases is inhibiting the transition from *I4/mcm* to *Ibmm*, which should occur if equilibrium were achieved.

Samples of $BaPb_{1-x}Bi_xO_3$ are generally prepared at a temperature where they would have a cubic structure. Thus, samples of orthorhombic $BaPb_{1-x}Bi_xO_3$ will have undergone two phase transitions on cooling to room temperature. The cubic –to-tetragonal transition is expected to produce a microstructure based on twining where the *c* axis in different domains will be along three different orthogonal directions of the cubic cell. This twining is made very likely by the fact that right at the transition temperature, there is no strain at the boundary between twins. Strain only develops below this transition as *c* slowly becomes shorter than *a* and *b*. The transition from tetragonal-to-orthorhombic is discontinuous so that strain due to expected twining will occur instantaneously when the transition occurs. Possibly, this strain could inhibit the tetragonal-to-orthorhombic from occurring in some regions of a sample.

2. Tilt angle and distortion of MO_6 octahedra Anomalous behavior of the tilt angle vs *x* for $BaPb_{1-x}Bi_xO_3$ phases was previously noted [16]. This is shown in Fig. S14. This figure differs somewhat from that previously shown. The octahedra tilt angle can be calculated from both O1 and O2 positions in the case of the *Ibmm* phase, and only one of these values was used in ref. 10. Both of these values were used here using the software Tubers [18]. These values were then averaged for use in Fig. S13. This does not greatly change the plot from what was previously given in ref. 10. The dashed line added to Fig. S14 could be considered the expected behavior. Note that this curve of tilt angle vs *x* then has the same shape as the phase boundary lines for the $BaPb_{1-x}Bi_xO_3$ phases shown in Fig. 7 of the main paper. Such a common shape would be expected because tilt angle should decrease as transition temperatures decrease. This common shape qualitatively validates the shape of the phase boundary lines in Fig. 7 of the main paper.

Significant deviations from the expected behavior of the tilt angle occur in the region where superconductivity occurs. One real possibility is that determined tilt angle values in the region where 2 phases coexist are simply incorrect. Although the Rietveld approach of refining structures from diffraction patterns with overlapping peaks is powerful, it is not infallible. This $BaPb_{1-x}Bi_xO_3$ system presents a special challenge because the two phases present both have a small distortion of the same basic structure, and the unit cell volumes of the two phases present is essentially the same. The tilt angle is based on the intensity of the relatively weak superlattice peaks, the peaks that would not occur if the tilting did not occur. The parameters used to fit peaks are dominated by the primary peaks, and these may not be completely reliable for the superlattice peaks. A complicating factor is lattice strain, which is known to be significant. Lattice strain is evident even at $x = 0.0$, where the

strain is anisotropic causing some peaks to broaden more than others [3,19]. Superlattice peaks for some perovskite compounds are broader than primary peaks and have positions displaced from those expected based on the fit of the primary peaks [20]. Superstructure peaks have been observed in a sample of $Ba_{1-x}K_xBiO_3$ at an *x* value of 0.25 due to ordering of Ba and K [21]. If some order of Pb and Bi is occuring at $x \sim 0.25$, this would produce weak superstructure peaks overlapping peaks due to tilting [22]. This could cause the high tilt angle values for *Ibmm* phases at 0.20 and 0.25 *x*, and the high tilt angle value for the 0.3*x I4/mcm* phase. Another issue is that isotropic displacement factors (U values) were used in the refinements [9,16]. It is well known that the thermal displacements of O perpendicular to the M-O-M linkage are much larger than along the M-O-M linkage. The fact that anisotropic Us were not used by either group is likely for the very good reason that this would have been more parameters than can be justified in this complex situation. However, it is the M-O-M angle that changess when the MO_6 octahedra tilt, and there will be some correlation between thermal motion perpendicular to the M-O-M linkage and the disordered tilt angle caused by the fact that Bi-O-Bi, Bi-O-Pb, and Pb-O-Pb angles will not have exactly the same values.

The other real possibility is that the anomalous tilt angles based on the reported Rietveld refinements are essentially correct, especially since two independent studies obtained very similar results [9,16]. The interdependence of the structure parameters is such that an anomaly in the tilt angle means that there must be an anomaly elsewhere in the structural parameters. In the case of the *Ibmm* phases, this is mainly in the O-M-O angles (Fig. S14). This deviation of a second angle from the ideal value of 90° for $x = 0.2$ and 0.25 is directly related to the tilt angle jump in Fig. S13. For a $BaPb_{0.8}Bi_{0.2}O_3$ sample, there is also data at 10 K showing that this increased distortion of the MO_6 octahedron remains at low temperature [9]. In the case of *I4/mcm* $BaPb_{0.7}Bi_{0.3}O_3$, the O-M-O angles are all fixed by symmetry at their ideal values of 90 and 180°. Here the anomaly at $x = 0.3$ is with the M-O distances of the MO_6 octahedra that are related to the high tilt angle found for this phase (Fig. S15). The M-O distances in the *Ibmm* and *I4/mcm* $BaPb_{1-x}Bi_xO_3$ phases are essentially equal to one another for a given value of *x*, except for *I4/mcm* $BaPb_{0.7}Bi_{0.3}O_3$ where the 2 M-O distances along the *c* axis and the 4 M-O distances perpendicular to the *c* axis are 2.154 and 2.163 Å (Fig. S14). This difference is large compared to those of all other *Ibmm* and *I4/mcm* phases in this system. We can be confident that this anomaly for the M-O distances is real because it is also reflected in the cell edges (Fig. S16), which are known to much higher accuracy than distances impacted by refined positional parameters. Plots of cell edges vs *x* show the magnitude of the *c* cell edge is slightly smaller than expected. This confirms the small compression of the MO_6 octahedra along the *c* axis, something that only occurs for *I4/mcm* $BaPb_{0.7}Bi_{0.3}O_3$. However, this distortion is actually more of an expansion perpendicular to the *c* axis. This does cause an expansion in the *a* cell edge because it is compensated by the octahedra tilt.

The value of the M-O distance along the c axis given in ref. 10 is wrong based on the crystallographic information given. The value given in Table II of that reference is

2.140 Å, which infers a much larger compression along the *c* axis relative to the correct value of 2.158 Å. This distance is exactly equal to the *c* cell edge divided by four. The value of 2.148 Å was erroneously based on the *c* cell edge of *Ibmm* $BaPb_{0.7}Bi_{0.3}O_3$ (8.56067 Å) instead of *I4/mcm* $BaPb_{0.7}Bi_{0.3}O_3$ (8.63106 Å).

The apparent distortions of the MO_6 octahedra occurring for $BaPb_{1-x}Bi_xO_3$ samples where $x = 0.2 – 0.3$ require further investigation to understand any possible relationship to the superconductivity in the $BaPb_{1-x}Bi_xO_3$ system.

References

1. R. B. Macquart, B.J.Kennedy, M. Avdeev, J. Solid State Chem. 183 (2010) 249–254.

2. W.T. Fu, D. Visser, K.S. Knight, D.J.W. IJdo, J. Solid State Chem. 177 (2004) 1667–1671.

3. W.T. Fua, D. Visser, K.S. Knight, D.J.W. IJdo, J. of Solid State Chem. 180 (2007) 1559–1565.

4. G. J. Thorogood, Maxim Avdeev, Melody L. Carter, Brendan J. Kennedy, J. Ting, K. S. Wallworkd, Dalton Trans., 40 (2011) 7228-7233.

5. B. J. Kennedy, B. A. Hunter, J. R. Hester, Phys. Rev. B65 (2002) 224103.

6. M. Glerup, K. S. Knight, F.W. Poulsen, Mat. Res. Bull. 40 (2005) 507–520.

7. C. J. Howard, K, S. Knight, B.J. Kennedy, E.H. Kisi, J. Phys.: Condens. Matter 12 (2000) L677–L683.

8. C.J. Howard, H.T. Stokes, Acta Crystallogr. B54 (1998) 782.

9. D. T. Marx, P. G. Radaelli, J. D. Jorgensen, R. L. Hitterman, D. G. Hinks, S. Pei, B. Dabrowski, Phys. Rev. B46 (1992)1144-1156.

10. L. Li, B. J. Kennedy, Y. Kubota, K. Kato, R. F. Garrett, J. Mater. Chem., 14 (2004) 263–273.

11. B.J. Kennedy, C.J. Howard, G.J. Thorogood, J.R. Hester, J. Solid State Chem. 161 (2001) 106-112.

12. E.H. Mountstevens, J.P. Attfield, S.A.T. Redfern, J. Phys.: Condens. Matter 15 (2003) 8315–8326.

13. W.T. Fu, D.J.W. IJdo, J. Solid State Chem. 179 (2006) 2732–2738

14. K. Knízek, J. Hejtmánek, Z. Jirak, C. Martin, M. Hervieu, B. Raveau, G. Andre, F. Bourée, Chem. Mater. 16 (2004) 1104-1110.

15. A.W. Sleight, D.E. Cox, Solid State Commun. 58 (1986) 347-350.

16. E. Climent-Pascual, N. Ni, S. Jia, Q. Huang, R. J. Cava, Phys. Rev. B 83 (2011) 174512.

17. O. Moretzki, T. Doering, M. Steins, M. Wendschuh-Josties, K. , Bente, Z. Kristallogr. NCS 215 (2000) 465-466.

18. M.W. Lufaso, P.M. Woodward, Acta Cryst., B57 (2001) 725.

19. D.E. Cox, A.W. Sleight, Proceedings of the Conference on Neutron Scattering (1976) 45-54.

20. P. Woodward, R.D. Hoffmann, A.W. Sleight, J. Mater. Res. 9 (1994) 2118–2127.

21. M.H.K. Rubel, A. Miura, T. Takei, N. Kumada, M. M. Ali, M. Nagao, S. Watauchi, I. Tanaka, K. Oka, M. Azuma, E. Magome, C. Moriyoshi, Y. Kuroiwa, A. K. M. A.Islam, Superconducting Double Perovskite Bismuth Oxide Prepared by a Low-Temperature Hydrothermal Reaction, Angew. Chem. Int. Ed., 53 (2014) 3599 –3603.

22. P.W. Barnes, M.W. Lufaso, P.M. Woodward, Acta Cryst. B62 (2006) 384-396.

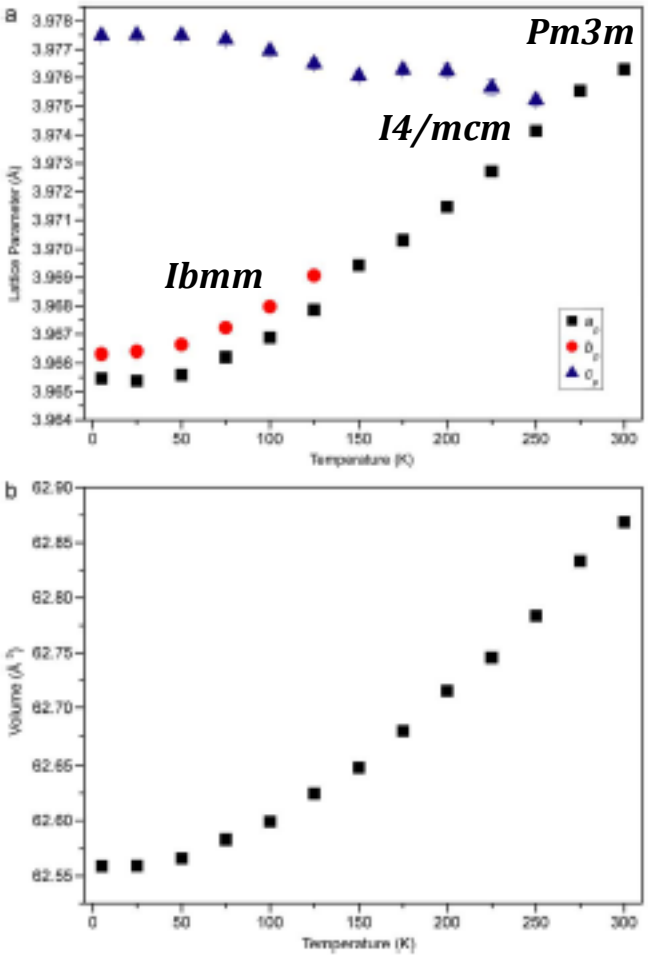

Fig. S1. Reduced cell dimensions vs temperature for $SrMoO_3$ [1]

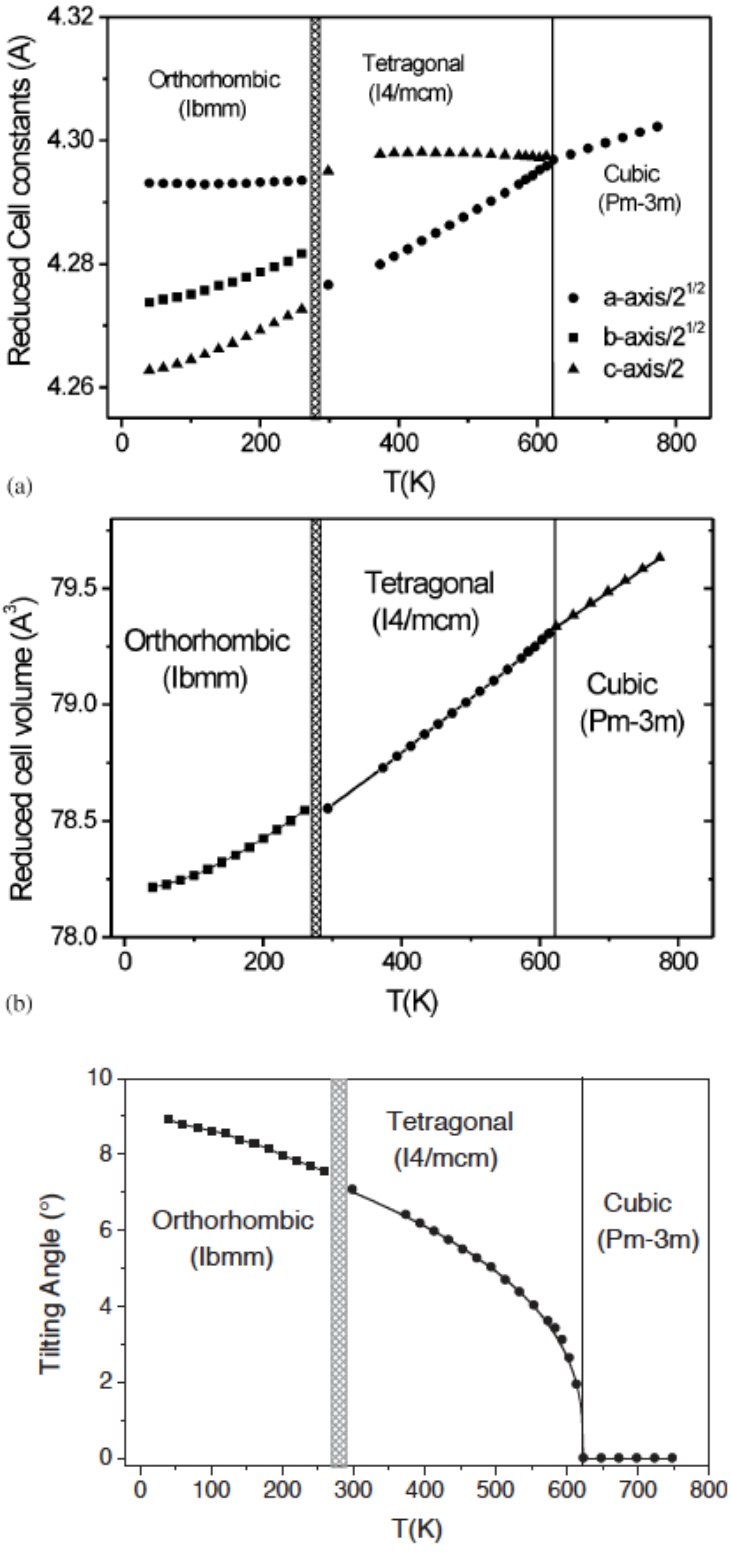

Fig. S2. $BaTbO_3$ reduced cell edges, volume, and tilt angles vs temperature [2].

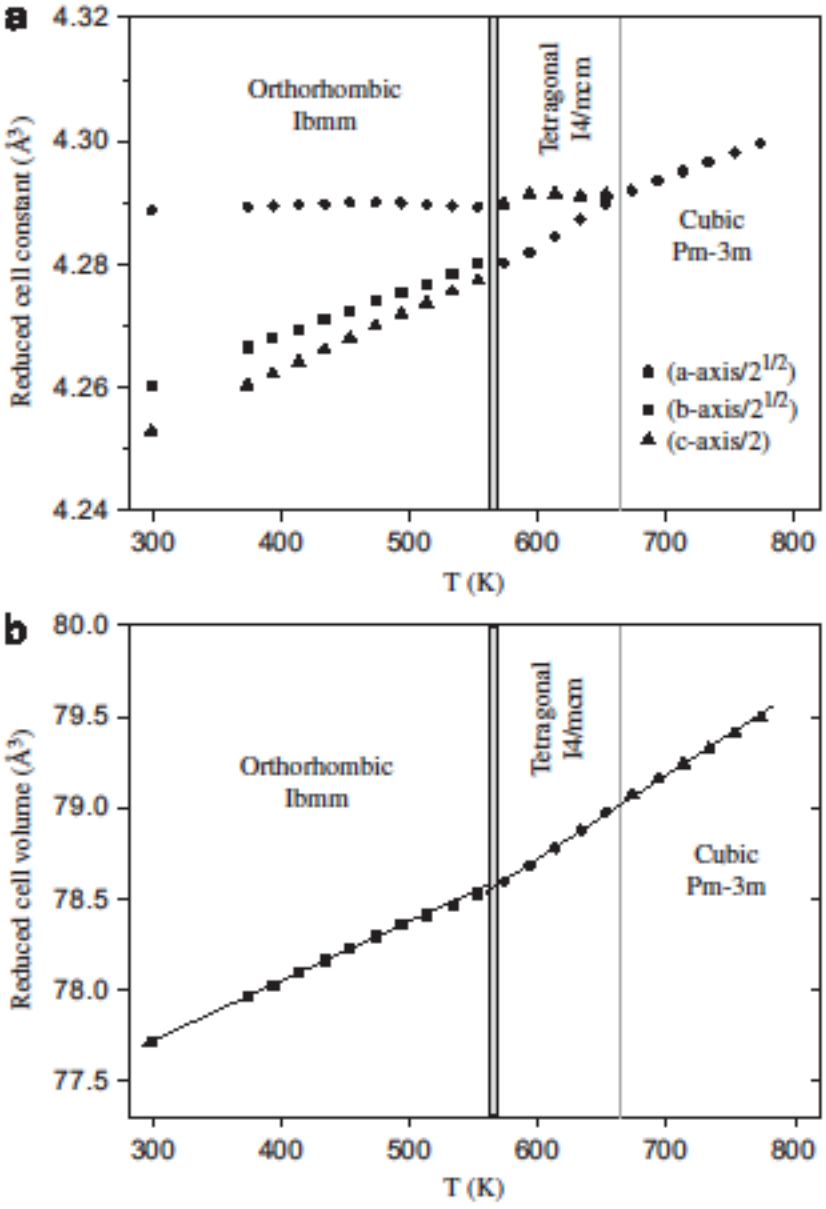

Fig. S3. Reduced cell edges and volume vs temperature for $BaPbO_3$ [3].

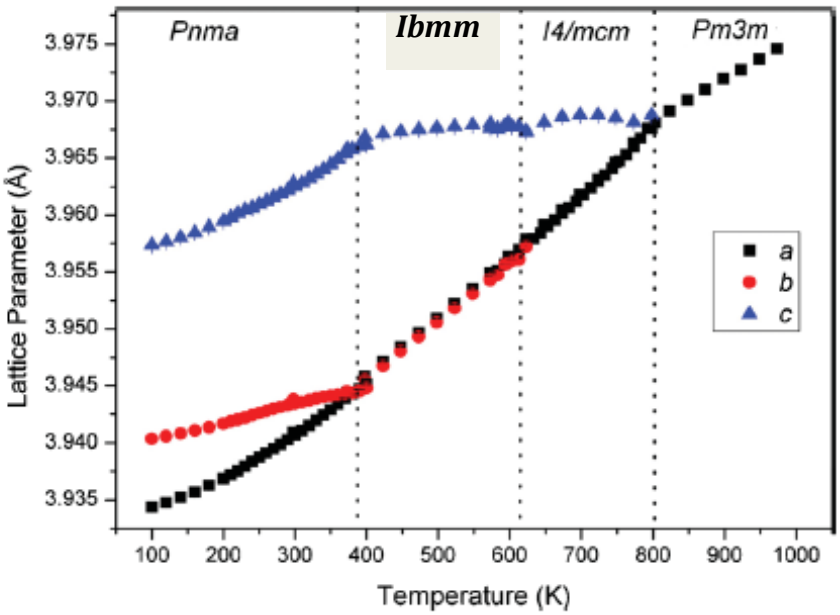

Fig. S4. Reduced cell dimension vs temperature for $SrTcO_3$ [4].

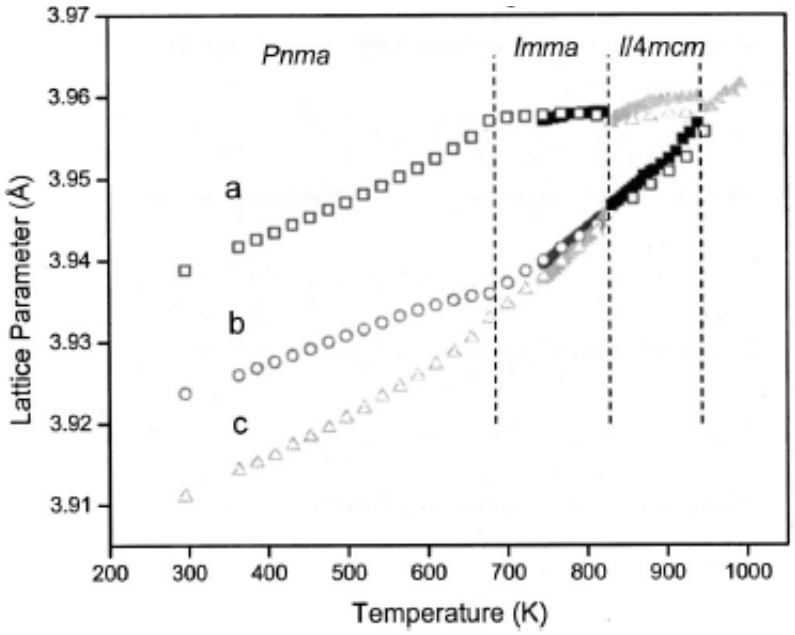

Fig. S5. Reduced cell dimensions vs temperature for $SrRuO_3$ [5]. Solid points are duplicate measurements. (*Imma* = *Ibmm*)

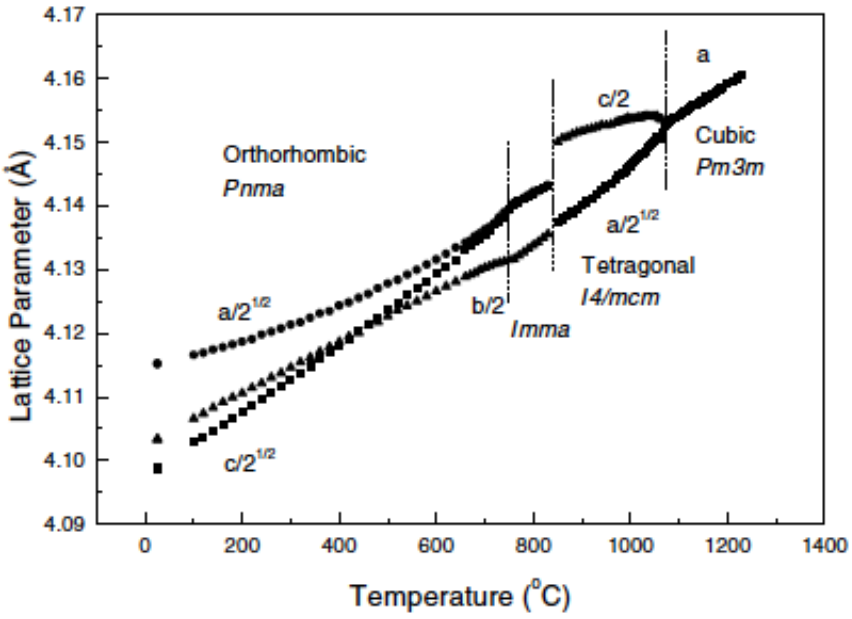

Fig. S6. Temperature dependence of reduced lattice parameters for $SrZrO_3$ [6]. (*Imma* = *Ibmm*)

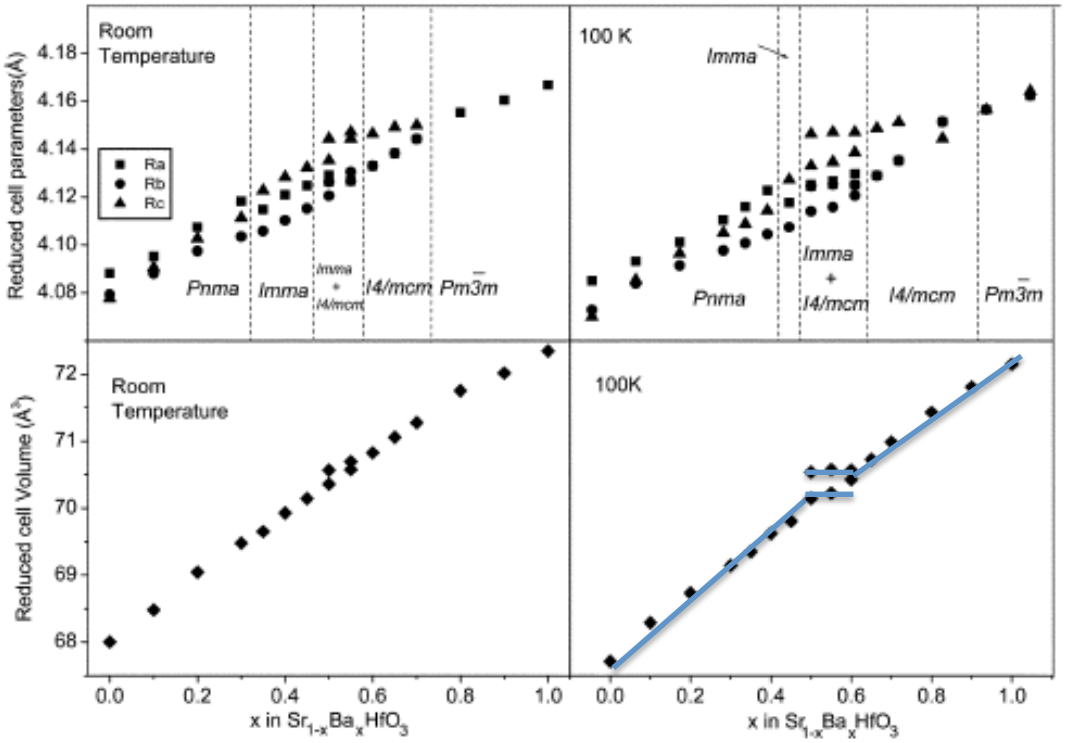

Fig. S7. Reduced cell parameters and volume vs temperature for $Sr_{1-x}Ba_xHfO_3$ phases [7]. Blue line indicates expected behavior for a miscibility gap. (I*mma* = *Ibmm*)

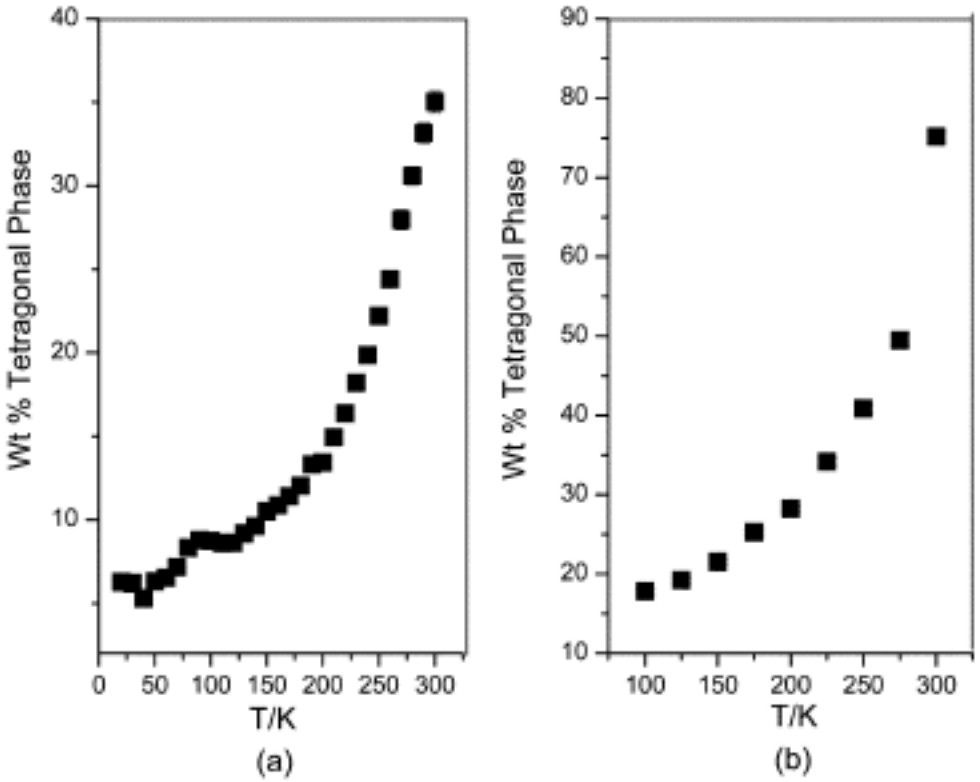

Fig. S8. Temperature dependence of the growth of the *I4/mcm* phase for (a) $Sr_{0.5}Ba_{0.5}HfO_3$ and (b) $Sr_{0.45}Ba_{0.55}HfO_3$.

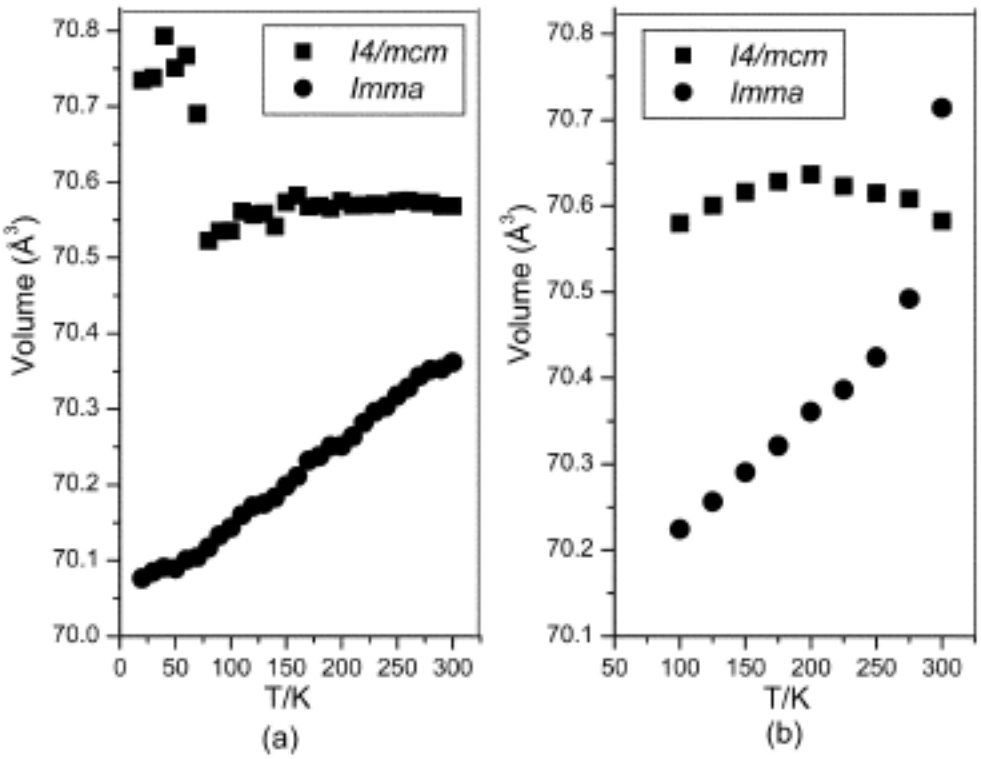

Fig. S9. Temperature dependence of the reduced cell volumes of the *Ibmm* (= *Imma*) and *I4/mcm* phases in (a) $Sr_{0.5}Ba_{0.5}HfO_3$ and (b) $Sr_{0.45}Ba_{0.55}HfO_3$ [9].

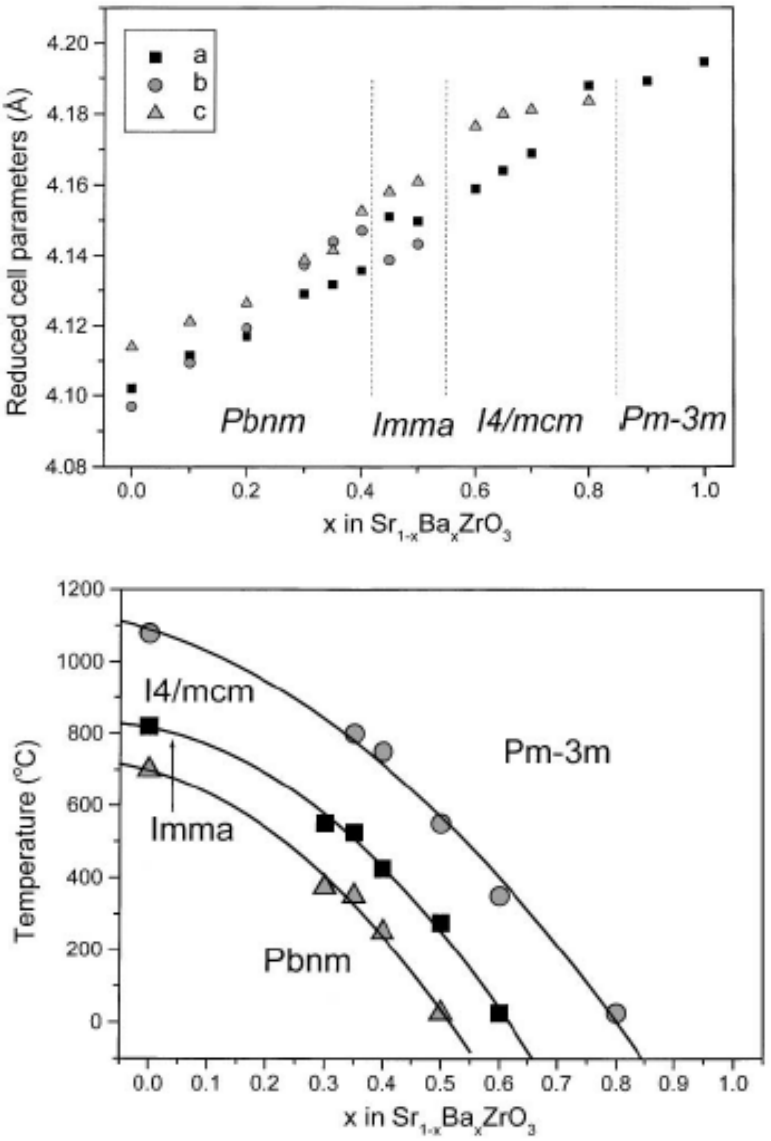

Fig. S10. Upper: Reduced cell parameters vs *x* for $Sr_{1-x}Ba_xZrO_3$ phases at 298 K. Lower: Phase diagram for the $Sr_{1-x}Ba_xZrO_3$ system [10]. (*Imma* = *Ibmm*)

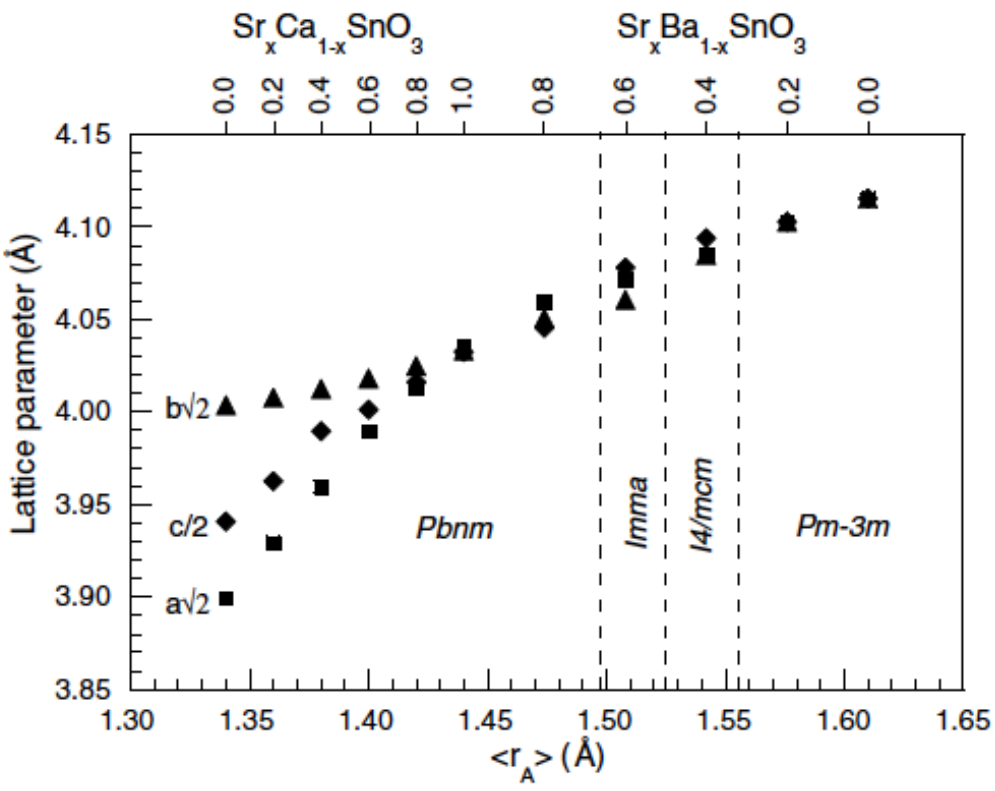

Fig. S11. Variation of reduced lattice parameters for $Sr_xCa_{1-x}SnO_3$ and $Sr_xBa_{1-x}SnO_3$ phases. (*Imma* = *Ibmm*)

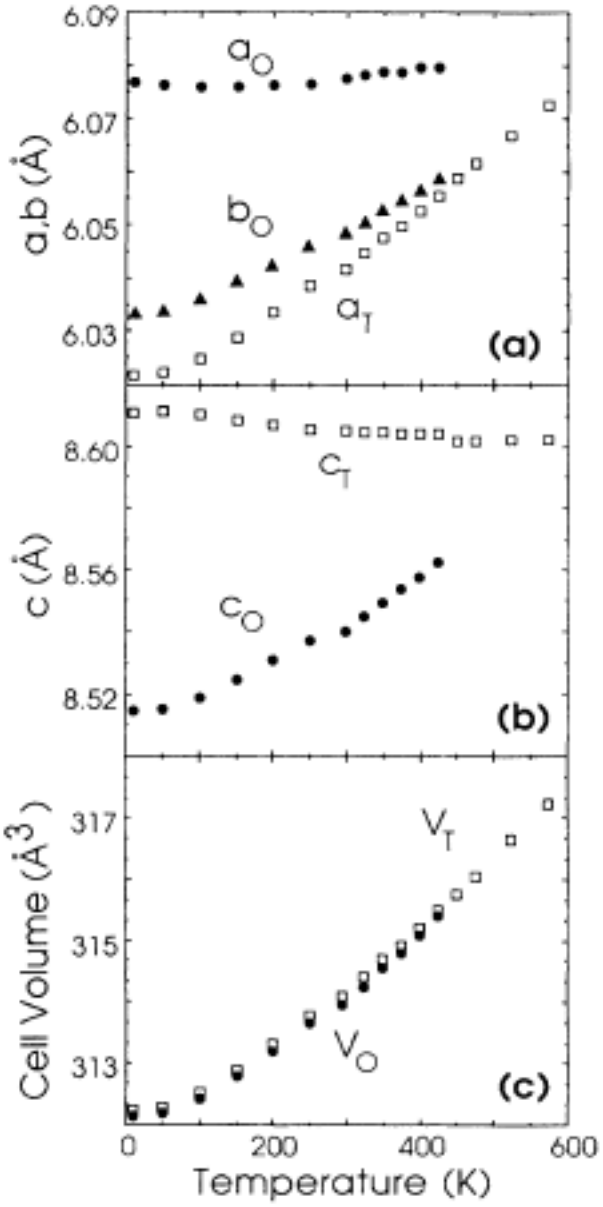

Fig. S12. Reduced cell edges and volume of a mixed tetragonal (T, open squares) and orthorhombic (O, filled circles) sample of composition $BaPb_{0.8}Bi_{0.2}O_3$ [9].

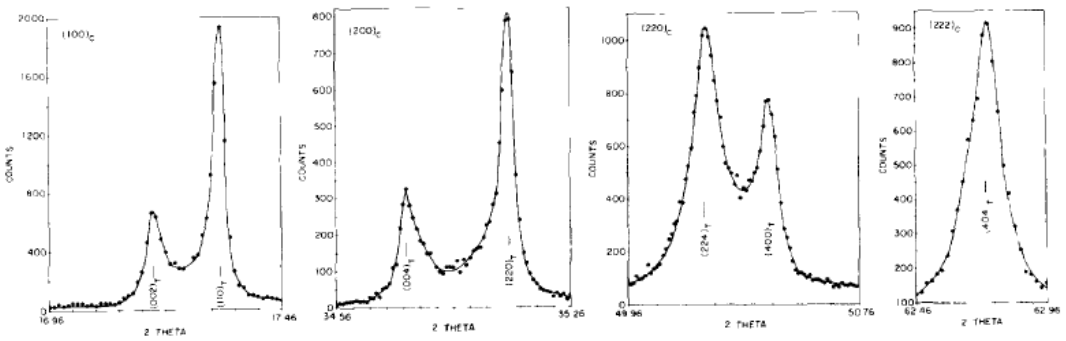

Fig. S13. Synchrotron X-ray diffraction data for a rapidly quenched sample of $BaPb_{0.725}Bi_{0.275}O_3$ [10]. This pattern was fit to a tetragonal cell with a = 6.0545 Å and c = 8.633 Å. No improvement in fit was obtained by adding an orthorhombic phase.

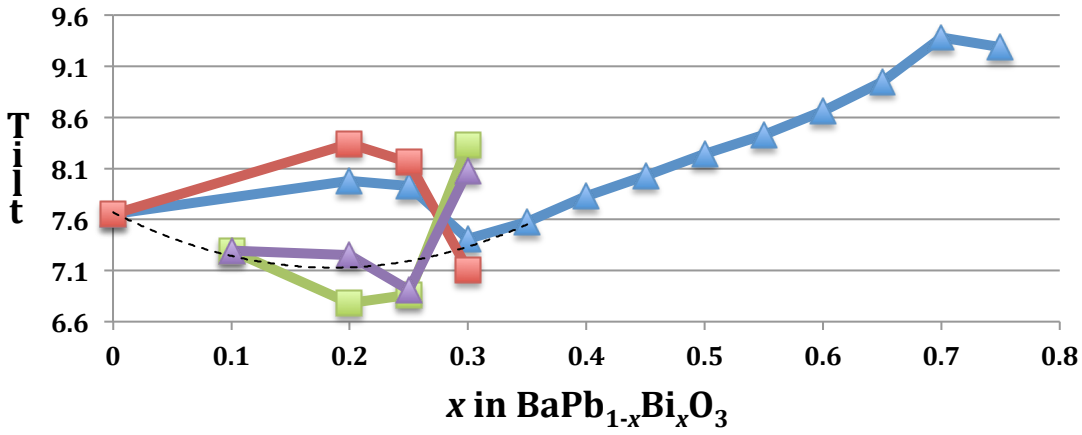

Fig. S14. Tilt angle vs *x* for $BaPb_{1-x}Bi_xO_3$ phases. Blue and red are for *Ibmm* phases, and green and violet are for *I4/mcm* phases. The dashed line connected to the blue line from 0.35 to 0.75 *x* can be considered as the expected behavior if distortions of MO_6 octahedra were very small. The shape of this expected behavior matches the shape of the phase boundary lines in Fig. 7 of the main paper. The large deviations from the expected behavior can be attributed to distortions of the MO_6 polyhedra shown in Figs. S15 and 16. Blue and violet data from ref. 9; red and green data from ref. 11, with the exception that data for the point at 0.1 *x* is from ref. 17.

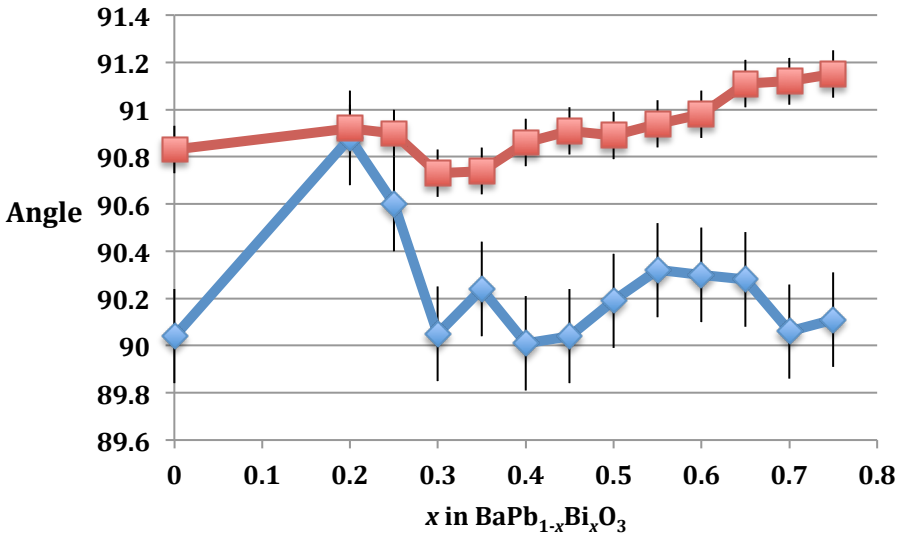

Fig. S15. The two O-M-O angles in orthorhombic $BaPb_{1-x}Bi_xO_3$ phases vs *x*, which ideally would be 90° for an undistorted MO_6 octahedron. The jump in one the O-M-O angles at $x = 0.2$ and 0.3 causes the jump in the tilt angles in Fig. S14. Data from ref. 9. Error bars are shown.

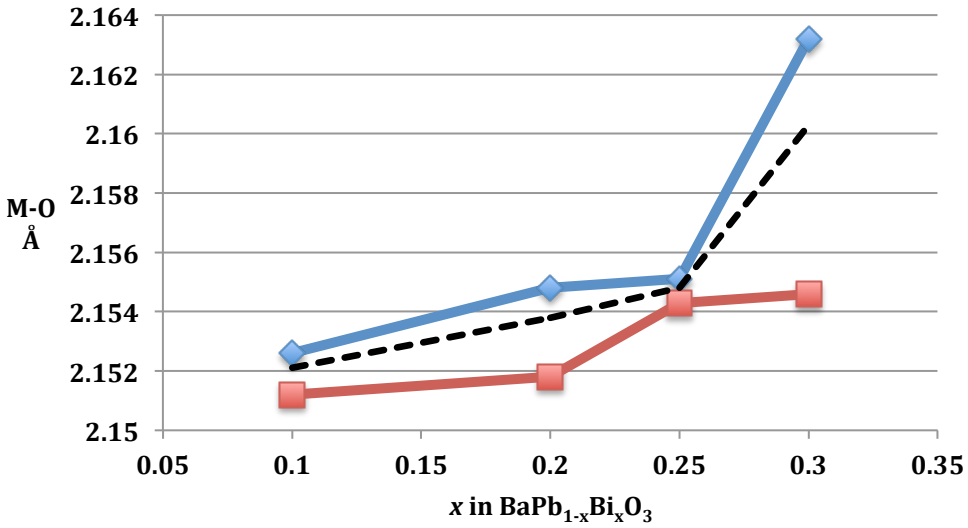

Fig. S16. The M-O distances in tetragonal $BaPb_{1-x}Bi_xO_3$ phases vs *x*. Data are from ref. 9, except for *x* = 0.1 where data are from a single crystal refinement [17]. There are 4 M-O distances in the *ab* plane (blue) and 2 M-O distances along *c* (red). The dashed line is the weighted average. All O-M-O angles are constrained by symmetry to be the ideal values of 90 and 180° in this tetragonal structure.

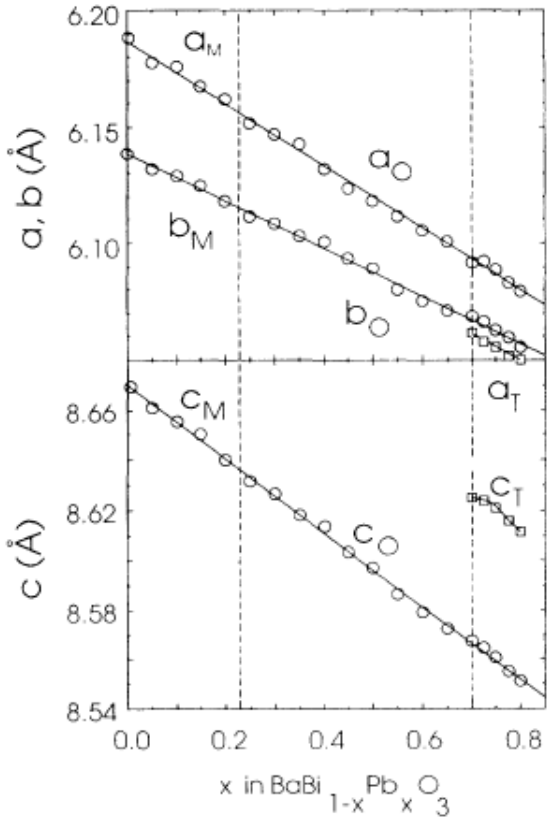

Fig. S17. Lattice constants vs composition where x is now Pb content [9].